

Improvement of the Thermoelectric Properties of $(\text{Sr}_{0.9}\text{La}_{0.1})_3\text{Ti}_2\text{O}_7$ by Ag Addition

G.H. Zheng · Z.H. Yuan · Z.X. Dai · H.Q. Wang ·
H.B. Li · Y.Q. Ma · G. Li

Received: 15 April 2013 / Accepted: 28 May 2013 / Published online: 8 June 2013
© The Author(s) 2013. This article is published with open access at Springerlink.com

Abstract Ruddlesden-Popper (RP) phase $(\text{Sr}_{0.9}\text{La}_{0.1})_3\text{Ti}_2\text{O}_7/x\text{Ag}$ ($x = 0, 0.05, 0.10, 0.15$) are systematically investigated with regard to their phase composition and thermoelectric transport properties. The XRD results show that all oxide samples are of two phases and they have layered microstructure. The electrical conductivity is found to be increased simultaneously. And the absolute Seebeck coefficient decreases firstly and then increases Ag addition, which leads to $(\text{Sr}_{0.9}\text{La}_{0.1})_3\text{Ti}_2\text{O}_7/x\text{Ag}$ ($x = 0.10$) sample possesses optimum power factor. The total thermal conductivity lowers with Ag addition. The dimensionless figure of merit, ZT , reaches 0.12 for $x = 0.10$. These results suggest that a proper of metal element Ag addition would be an effective way improving thermoelectric performance of $(\text{Sr}_{0.9}\text{La}_{0.1})_3\text{Ti}_2\text{O}_7$ system.

Keywords Ag addition · Oxide materials · Thermoelectric performance

1 Introduction

Thermoelectric materials have been attracted much attention for which can convert thermal energy to electrical energy [1–3]. Its efficiency was evaluated by the thermoelectric figure of merit $ZT = S^2\sigma T/\kappa$, where S , σ , T , and κ represent absolute Seebeck coefficient, electrical conductivity, temperature, and thermal conductivity, respectively. Obviously, a good thermoelectric material should possess a larger Seebeck coefficient S , high electrical conductivity σ , and low thermal conductivity κ .

Recently oxide thermoelectric materials (e.g. $\text{Ca}_3\text{Co}_4\text{O}_9$, LaCoO_3 , and SrTiO_3) [4–6] are received much interest because they are environmental friendly and basically stable at high temperatures. Among them, carrier-doped SrTiO_3 is a promising

G.H. Zheng (✉) · Z.H. Yuan · Z.X. Dai · H.Q. Wang · H.B. Li · Y.Q. Ma · G. Li
Anhui Key Laboratory of Information Materials and Devices, School of Physics and Material Science, Anhui University, Hefei 230039, People's Republic of China
e-mail: ghzheng@ahu.edu.cn

candidate of n -type oxide, because it exhibits rather large Seebeck coefficient S [7]. Lanthanum doped SrTiO_3 single crystal exhibits high power factor comparable with that of Bi-Te alloy at room temperature [8, 9]. However, their thermoelectric performance is still low due to the fact that the κ value of SrTiO_3 bulk crystal (~ 12 W/mK) [10] at room temperature is approximately one order of magnitude larger than that of Bi_2Te_3 [8]. In order to efficiently reduce the κ value of SrTiO_3 , one way is its layered perovskite-type $\text{SrO}(\text{SrTiO}_3)_n$ or $\text{Sr}_{n+1}\text{Ti}_n\text{O}_{3n+1}$ ($n = \text{integer}$) termed as Ruddlesden-Popper (RP) phase [11, 12], which have a layered structure composed of alternate stacks of rock salt SrO layer and perovskite $(\text{SrTiO}_3)_n$ block layer along the c -axis. This layer structure can exhibit rather low κ values because phonon scattering occurs efficiently at the interface between SrO layer and $(\text{SrTiO}_3)_n$ block layer. Very recently, a proper of Ag added in $\text{Ca}_3\text{Co}_4\text{O}_{9+\delta}$ ceramics resulted in an increase of the power factor, since Ag could improve electrical connections between cobaltite grains resulting in a significant increase in σ without largely increasing κ [13, 14]. In addition, according to the reference [15], in the semiconducting matrix, metallic addition induces band bending which creates a potential barrier. Such a barrier acts as an energy filter from which low-energy electrons are strongly scattered, while high-energy electrons remain almost unaffected. This filtering effect increases the mean energy per carrier resulting in the Seebeck coefficient larger.

Encouraged by these results, we attempt to improve the thermoelectric performance for the Ruddlesden-Popper phases $(\text{Sr}_{0.9}\text{La}_{0.1})_3\text{Ti}_2\text{O}_7$ ceramic by Ag addition. In this paper, $(\text{Sr}_{0.9}\text{La}_{0.1})_3\text{Ti}_2\text{O}_7/x\text{Ag}$ ($x = 0, 0.05, 0.10$ and 0.15) samples have been prepared by hydrothermal method and heated. Thermoelectric properties have been measured in temperature range from 250 K to 1050 K, and the effects of Ag addition on thermoelectric properties $(\text{Sr}_{0.9}\text{La}_{0.1})_3\text{Ti}_2\text{O}_7$ ceramic have been discussed.

2 Experimental

The $(\text{Sr}_{0.9}\text{La}_{0.1})_3\text{Ti}_2\text{O}_7/x\text{Ag}$ ($x = 0, 0.05, 0.10$ and 0.15) composites were synthesized via a hydrothermal method and heated. First, high-purity strontium, lanthanum, and silver nitrate were dissolved in deionized water and tetrabutyl titanate was dissolved in ethanol to form uniform solutions. Subsequently, the latter solution was added dropwise into the Sr, La, and silver nitrate solution under stirring, and the PH value of the mixed solution was adjusted to 13 by adding NaOH. After ultrasonic stirring, the solution was transferred into a Teflon autoclave followed by hydrothermal treatment at 200 °C for 48 h. After the autoclave cooled down to room temperature, the obtained products were washed several times with deionized water and ethanol, and then dried overnight. And then the products were pressed into compact pellets and annealed at 1450 °C for 4 h in a carbon crucible in the presence of argon gas with 5 mol% hydrogen.

The phase composition of as-prepared samples were characterized a Japanese company's MXP18AHF MARK X-ray diffraction over the 2θ range of 20°–80°. Squares of 10 mm \times 10 mm \times 2 mm and bars of about 2 mm \times 3 mm \times 12 mm were cut and polished from the pressed disks for characterization of the thermoelectric properties. The electrical resistivity of the sample was measured by a four-point direct current (DC) current-switching technique, and the Seebeck coefficient

was measured by a static DC method, using commercial equipment (ZEM-3(M10), Ulvac Riko, Inc.) in a low-pressure helium environment with temperatures ranging from 250 K to 1050 K. The thermal diffusivity D was measured using the laser flash method (Netzsch, LFA 457). The specific heat C_p was determined by a commercial instrument (Q2000DSC, AmericaTa). The density ρ was measured by Archimedes' method. The resulting thermal conductivity was calculated from the measured thermal diffusivity D , specific heat C_p , and density ρ from the relationship $\kappa = D\rho C_p$.

3 Results and Discussion

The powder X-ray diffraction for $(\text{Sr}_{0.9}\text{La}_{0.1})_3\text{Ti}_2\text{O}_7/x\text{Ag}$ ($x = 0, 0.05, 0.10$ and 0.15) are presented in Fig. 1. It can be seen that the $(\text{Sr}_{0.9}\text{La}_{0.1})_3\text{Ti}_2\text{O}_7$ sample contains single phase and no detectable impurity phase appears, indicating that La is doped into the lattice without obvious change in the crystal structure. In addition, Ag-added samples are composed of $(\text{Sr}_{0.9}\text{La}_{0.1})_3\text{Ti}_2\text{O}_7$ and metallic Ag. Although the X-ray diffraction peaks (at $2\theta = 38.1^\circ, 44.3^\circ, 53.8^\circ$ and 64.5°) of Ag are well overlapped with those for $(\text{Sr}_{0.9}\text{La}_{0.1})_3\text{Ti}_2\text{O}_7$, these peaks become stronger and stronger with the increasing in Ag content. This indicates these four peaks are well related to silver, and that Ag precipitates as a second phase in these samples.

Figure 2 shows the temperature dependence of the electrical conductivity $\sigma(T)$ for the compositions of $(\text{Sr}_{0.9}\text{La}_{0.1})_3\text{Ti}_2\text{O}_7/x\text{Ag}$ ($x = 0, 0.05, 0.10$ and 0.15) measured in the temperature range from 250 K to 1050 K. The electrical conductivity decreases with increasing temperature for all samples in the measured temperatures range, showing a typical metallic behavior. The electrical conductivity increases slightly with increasing Ag addition content, the same phenomena has also been observed in the Ag added in $\text{Ca}_3\text{Co}_4\text{O}_{9+\delta}$ ceramic [16]. This phenomenon can be ascribed to the two following reasons. On the one hand, Ag addition causes an increase in carrier concentration, and, on the other hand, Ag can act as electrical connections between $(\text{Sr}_{0.9}\text{La}_{0.1})_3\text{Ti}_2\text{O}_7$ grains. As a result, the electrical conductivity for the

Fig. 1 XRD patterns of $(\text{Sr}_{0.9}\text{La}_{0.1})_3\text{Ti}_2\text{O}_7/x\text{Ag}$ ($x = 0, 0.05, 0.10$ and 0.15) compounds at the room temperature

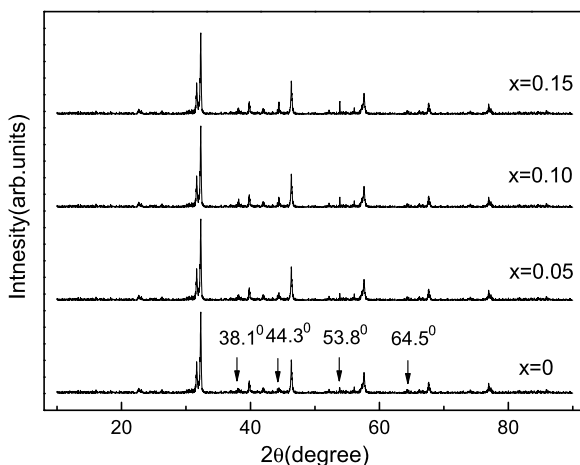


Fig. 2 Temperature dependence of the conductivity $\sigma(T)$ of the compound $(\text{Sr}_{0.9}\text{La}_{0.1})_3\text{Ti}_2\text{O}_7/x\text{Ag}$ ($x = 0, 0.05, 0.10, \text{ and } 0.15$)

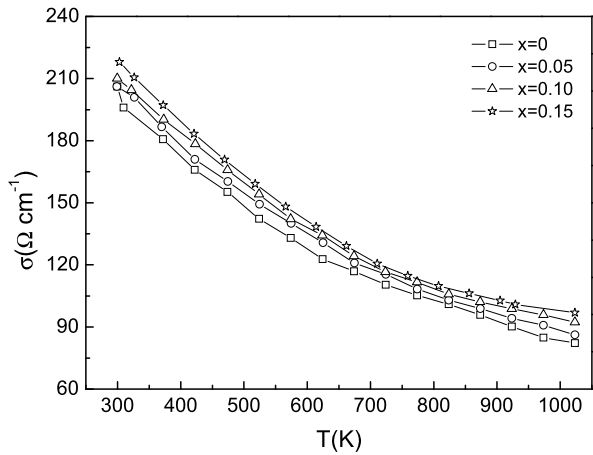
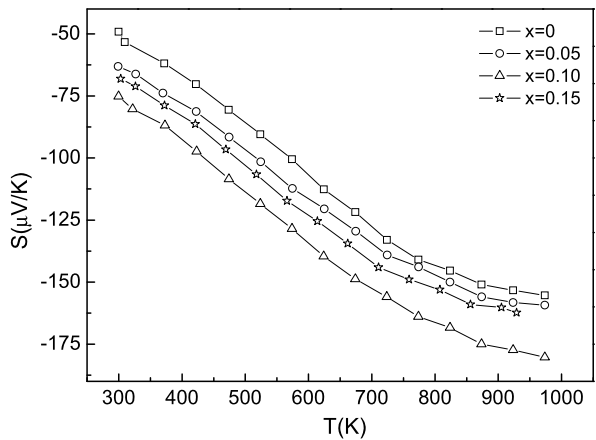


Fig. 3 Temperature dependence of Seebeck coefficient $S(T)$ of the compound $(\text{Sr}_{0.9}\text{La}_{0.1})_3\text{Ti}_2\text{O}_7/x\text{Ag}$ ($x = 0, 0.05, 0.10, \text{ and } 0.15$)

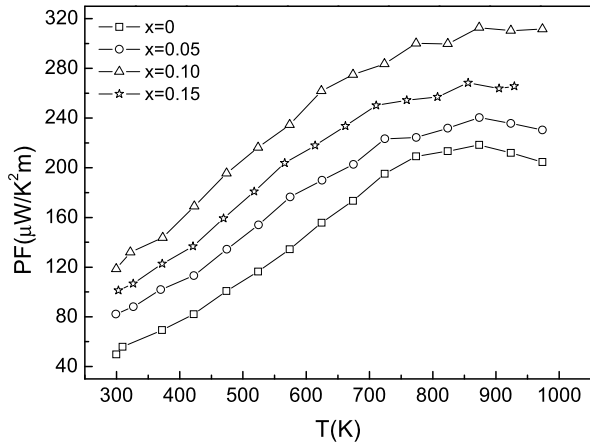


$(\text{Sr}_{0.9}\text{La}_{0.1})_3\text{Ti}_2\text{O}_7/x\text{Ag}$ ($x = 0, 0.05, 0.10 \text{ and } 0.15$) compounds is enhanced with increasing Ag content.

The temperature dependence of Seebeck coefficient S of the $(\text{Sr}_{0.9}\text{La}_{0.1})_3\text{Ti}_2\text{O}_7/x\text{Ag}$ ($x = 0, 0.05, 0.10 \text{ and } 0.15$) composites is shown in Fig. 3. The Seebeck coefficient for all samples is negative in the measured temperature range, which indicates that the dominant carriers are electrons. In addition, the absolute Seebeck coefficient $|S|$ for $(\text{Sr}_{0.9}\text{La}_{0.1})_3\text{Ti}_2\text{O}_7/x\text{Ag}$ increases monotonically with increasing temperature showing a metallic behavior, which is accordance with the electrical conductivity behaviors as shown in Fig. 2.

The absolute Seebeck coefficient $|S|$ of the composites increases with Ag content from $x = 0$ to 0.10, and then decreases when Ag content reaches to 0.15, as shown in Fig. 3. According to the reference [15], a potential barrier will appear induced by band bending when metallic addition in the semiconductor matrix. Such a barrier acts as an energy filter from which low-energy electrons are strongly scattered, while high-energy electrons remain almost unaffected. This filtering effect increases the mean energy per carrier resulting in enhanced $|S|$. Therefore, in our

Fig. 4 Temperature dependence of power factor PF of the compound $(\text{Sr}_{0.9}\text{La}_{0.1})_3\text{Ti}_2\text{O}_7/x\text{Ag}$ ($x = 0, 0.05, 0.10, \text{ and } 0.15$)

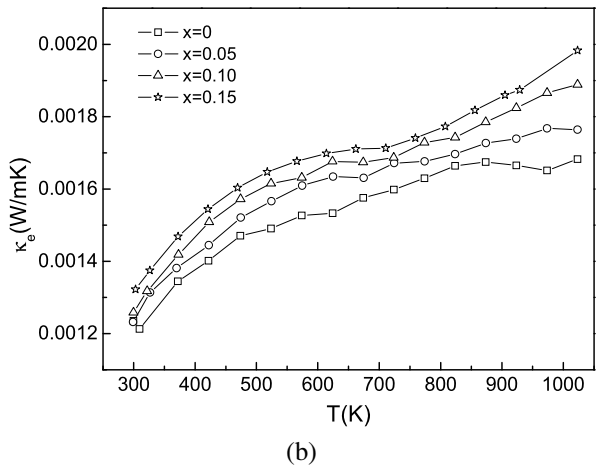
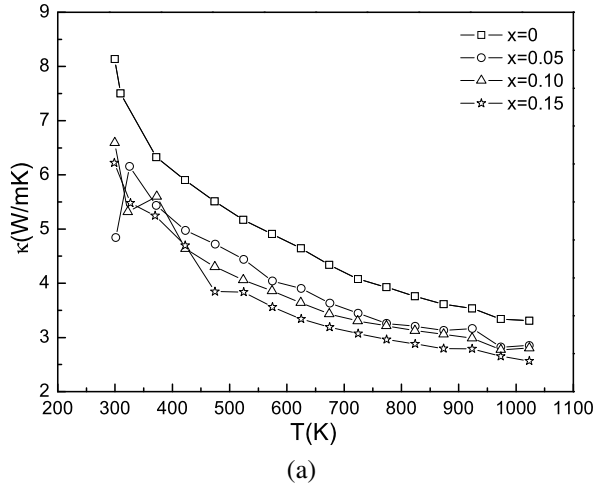


samples $(\text{Sr}_{0.9}\text{La}_{0.1})_3\text{Ti}_2\text{O}_7$ matrix, Ag addition maybe induce the filtering of low energy carriers at the matrix/inclusion interfaces, resulting in the enhancement of $|S|$ from $x = 0$ to 0.10. However, it can be noticed that with a further increase in Ag content, $|S|$ decreases as shown in Fig. 3. As indicated in the reference [15], the contribution of island scattering becomes the dominant factor for the larger values of interface potential, and Seebeck coefficient S will saturate when interface potential reaches a certain value. However, for our sample $x = 0.15$, Ag particles may be clustered, the voltage between $(\text{Sr}_{0.9}\text{La}_{0.1})_3\text{Ti}_2\text{O}_7$ particles, which are bridged via the clustered Ag particles, becomes smaller correspondingly, as a result, Seebeck coefficient S becomes smaller comparing with that for $x = 0.10$. So, when Ag content increases from $x = 0.10$ to 0.15, Seebeck coefficient $|S|$ becomes smaller.

Based on the above result, the PF (power factors) are calculated from $S^2\sigma$, and are presented in Fig. 4. With temperature increasing, PF firstly increases and reaches a maximum at 850 K, then decreases slightly with further increasing of temperature. Obviously, the general trend of temperature dependence does not changed by the Ag addition. The maximum of power factor values for $x = 0, 0.05, 0.10, \text{ and } 0.15$ samples are $218 \mu\text{W}/\text{K}^2 \text{ m}$, $240 \mu\text{W}/\text{K}^2 \text{ m}$, $315 \mu\text{W}/\text{K}^2 \text{ m}$ and $275 \mu\text{W}/\text{K}^2 \text{ m}$, respectively. The $x = 0.10$ sample exhibits the highest power factor. This is result of the effectively increasing of electrical conductivity while increasing the Seebeck coefficient by Ag addition from $x = 0$ to 0.10 as discussed before. With increasing Ag content to $x = 0.15$, the PF values decreases, which is ascribed to the decrease of the Seebeck coefficient as shown in Fig. 3.

The temperature dependence of the total thermal conductivity is shown in Fig. 5(a) in temperature range from 250 K to 1050 K. The total thermal conductivity decreases with increasing temperature in the whole measurement temperature range. The higher the Ag content, the lower the total thermal conductivity. In our samples, Ag nanoinclusion becomes scattering centers in matrix SrTiO_3 to reducing thermal conductivity. Similar phenomena have been observed by adding TiO_2 , mesoporous silica, titanate nanotube [17–19].

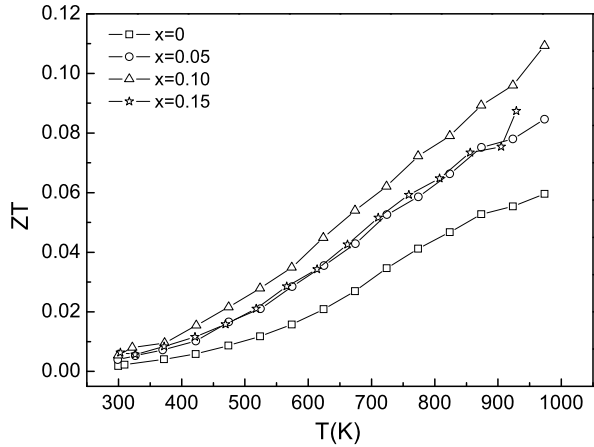
Fig. 5 Temperature dependence of total thermal conductivity $\kappa(T)$ and electronic thermal conductivity $\kappa_e(T)$ of the compound $(\text{Sr}_{0.9}\text{La}_{0.1})_3\text{Ti}_2\text{O}_7/x\text{Ag}$ ($x = 0, 0.05, 0.10,$ and 0.15)



The total thermal conductivity consists of a lattice contribution κ_p and a contribution from electrons, κ_e , i.e. $\kappa = \kappa_p + \kappa_e$. Usually, the electronic thermal conductivity κ_e is calculated from Wiedemann–Franz law as $\kappa_e = LT\sigma$, here L is Lorentz number, and $L = 2.44 \times 10^{-8} \text{ V}^2 \text{ K}^{-2}$ for free electrons. The relation between the electronic thermal conductivity and temperature is shown in Fig. 5(b). It can be seen that κ_e increases with increasing Ag content, which is ascribed to the increase of electrical conductivity as discussed in Fig. 4. Comparing with the total thermal conductivity, the electronic thermal conductivity is very small, which indicates that total thermal conductivity come mainly from the phonon scattering.

Temperature dependence of the dimensionless figure of merit ZT is shown in Fig. 6 for different Ag addition. It can be seen that ZT value for all samples increase with increasing temperature, and Ag addition enhances the figure of merit. The maximum figure of merit for $x = 0, 0.05, 0.10$ and 0.15 samples are 0.06, 0.08, 0.12 and 0.09, respectively. The $(\text{Sr}_{0.9}\text{La}_{0.1})_3\text{Ti}_2\text{O}_7/x\text{Ag}$ ($x = 0.10$) sample showed the

Fig. 6 Temperature dependence of ZT for the compound $(\text{Sr}_{0.9}\text{La}_{0.1})_3\text{Ti}_2\text{O}_7/x\text{Ag}$ ($x = 0, 0.05, 0.10, \text{ and } 0.15$)



largest ZT values among all the samples due to the large power factor as shown in Fig. 5.

4 Conclusions

We reported the thermoelectric properties for $(\text{Sr}_{0.9}\text{La}_{0.1})_3\text{Ti}_2\text{O}_7/x\text{Ag}$ ($x = 0, 0.05, 0.10$ and 0.15) composites fabricated by hydrothermal method and heated. The results indicated that Ag addition caused an increase in the electrical conductivity for owing to an increase in carrier concentration. With Ag addition, Seebeck coefficient $|S|$ increases and then decreases. The total thermal conductivity for $(\text{Sr}_{0.9}\text{La}_{0.1})_3\text{Ti}_2\text{O}_7/x\text{Ag}$ ($x = 0, 0.05, 0.10$ and 0.15) samples decreased with an increase in Ag content due to enhanced scattering of phonons. The maximum value of the figure of merit reached 0.12 for $x = 0.10$ sample, showing that Ag addition is a promising approach for enhancement of the thermoelectric performance for $(\text{Sr}_{0.9}\text{La}_{0.1})_3\text{Ti}_2\text{O}_7$.

Acknowledgements This work was financially supported by the National Science Foundation of China under Grant No. 11204001, No. 10804110 and No. 11174004; this work was also financially supported by Anhui Provincial Natural Science Foundation (1208085QA07); by Anhui University Scientific Research Fund No. 06060283, No. 2009QN006A and No. 32030028, '211 Project' of Anhui University.

Open Access This article is distributed under the terms of the Creative Commons Attribution License which permits any use, distribution, and reproduction in any medium, provided the original author(s) and the source are credited.

References

1. O. Berdan, E. Ahmet, A.M. Ali, J. Low Temp. Phys. **147**, 31 (2007)
2. O. Berdan, E. Ahmet, A.M. Al, J. Low Temp. Phys. **149**, 105 (2007)
3. G.H. Zheng, Z.X. Dai, Y.Q. Dong, Y.Y. Zhang, Y.Q. Ma, H. Zhang, G. Li, J. Low Temp. Phys. **165**, 43 (2011)

4. Y. Song, C.W. Nan, *Physica B* **406**, 2919 (2011)
5. Y. Song, Q. Sun, Y. Lu, X. Liu, F.P. Wang, *J. Alloys Compd.* **536**, 150 (2012)
6. J. Liu, H.C. Wang, W.B. Su, C.L. Wang, J.L. Zhang, L.M. Mei, *Solid State Sci.* **12**, 134 (2010)
7. H. Muta, K. Kurosaki, S. Yamanaka, *J. Alloys Compd.* **392**, 306 (2005)
8. T. Okuda, K. Nakanishi, S. Miyasaka, Y. Tokura, *Phys. Rev. B* **63**, 113104 (2001)
9. S. Ohta, T. Nomura, H. Ohta, K. Koumoto, *J. Appl. Phys.* **97**, 034106 (2005)
10. Y. Suemune, *J. Phys. Soc. Jpn.* **20**, 174 (1965)
11. S.N. Ruddlesden, P. Popper, *Acta Crystallogr.* **10**, 538 (1957)
12. S.N. Ruddlesden, P. Popper, *Acta Crystallogr.* **11**, 54 (1958)
13. Y. Song, Q. Sun, L.R. Zhao, F.P. Wang, *Mater. Sci. Forum* **650**, 132 (2012)
14. Y. Wang, Y.Sui.J. Cheng, X. Wang, W. Su, *J. Alloys Compd.* **477**, 817 (2009)
15. S.V. Faleev, F. Leonard, *Phys. Rev. B* **77**, 214304 (2008)
16. N.V. Nong, N. Pryds, S. Linderoth, M. Ohtaki, *Adv. Mater.* **23**, 2484 (2011)
17. N. Wang, L. Han, H.C. He, Y.S. Ba, K. Koumoto, *J. Alloys Compd.* **497**, 308 (2010)
18. N. Wang, H.C. He, X. Li, L. Han, C.Q. Zhang, *J. Alloys Compd.* **506**, 293 (2010)
19. W. Kim, J. Zide, A. Gossard, D. Klenov, S. Stemmer, A. Shakouri, A. Majumdar, *Phys. Rev. Lett.* **96**, 045901 (2006)